*Aust. J. Phys.*, 1986, **39**, 761–77

# Dynamics of Single- and Multi-photon Ionisation Processes in Molecules*

*V. McKoy, S. N. Dixit, R. L. Dubs and D. L. Lynch*

Arthur Amos Noyes Laboratory of Chemical Physics,
California Institute of Technology, Pasadena, CA 91125, U.S.A.

*Abstract*

Single-photon ionisation and resonant multiphoton ionisation studies, which can now be carried out using synchrotron radiation and pulsed dye lasers respectively, are providing important dynamical information on molecular photoionisation. In this paper we discuss some results of our recent studies of several single- and multi-photon ionisation processes in molecules. The results will be taken from our studies of (i) single-photon ionisation of linear molecules with emphasis on the role of shape and autoionising resonances on these cross sections, (ii) photoionisation from oriented NiCO as a simple but realistic model of photoemission in adsorbate–substrate systems, and (iii) resonant multiphoton ionisation of $H_2$.

## 1. Introduction

Single-photon and resonant multiphoton ionisation studies, which can now be carried out using the radiation provided by synchrotron sources and lasers respectively, are providing increasing amounts of important dynamical information on molecular photoionisation (Pratt *et al.* 1983; Dehmer *et al.* 1984). For example, the tunability, intensity, and wide spectral range of the radiation available from synchrotrons have made possible a large variety of photoionisation studies which would have been otherwise impossible (Winick and Doniach 1980). In addition to the many new and significant studies of shape and autoionising resonant features in photoionisation spectra which have thus become possible (Dehmer *et al.* 1984; McKoy *et al.* 1984), these properties of synchrotron radiation have opened up new areas of research capability in disciplines such as surface physics and catalytic chemistry (Winick and Doniach 1980). Furthermore, the technique of resonant multiphoton ionisation using pulsed dye lasers combined with photoelectron energy analysis is now being used to probe the dynamics of photoionisation of excited electronic states of molecules. A remarkable feature of photoelectron spectroscopy based on resonant multiphoton ionisation is that the excited state can be selected with respect to both vibrational and rotational levels by specific laser excitation. With this technique the spectroscopy and dynamics of the resonant excited state can be studied with very high resolution (Pratt *et al.* 1984*a*, 1984*b*; Bjerre *et al.* 1985) and intensities and photoelectron angular

* Paper presented at the Specialist Workshop on Excited and Ionised States of Atoms and Molecules, Strathgordon, Tasmania, 3–7 February 1986.

0004-9506/86/050761$02.00

distributions can now be measured for rotationally and vibrationally state-selected molecules (White *et al.* 1982; Anderson *et al.* 1984; Pratt *et al.* 1984*a*, 1984*b*; Kimura 1985). These and other properties make resonant multiphoton ionisation a versatile state-specific probe of molecules (Marinero *et al.* 1982; Zewail 1983 and references therein; Burns 1985).

In this paper we discuss some results of our recent studies of several single- and multi-photon ionisation processes in molecules. The results presented are taken from our studies of (i) single-photon ionisation of linear molecules with emphasis on the role of shape and autoionising resonances on these cross sections, (ii) photoionisation from oriented CO and NiCO as a simple but realistic model of photoemission in adsorbate–substrate systems, and (iii) resonant multiphoton ionisation of $H_2$.

An important objective of these studies is to enhance our ability to understand and predict the underlying dynamical content of molecular photoionisation data which are becoming increasingly available from synchrotron and laser sources. Although there are many important aspects of our formulation which are specific to the different ionisation processes, i.e. whether it is single- or multi-photon, a significant feature of our studies is that they are carried out using quantitative reliable wavefunctions for the molecular electronic continuum states. It is important to note that, while techniques for the determination of bound molecular electronic states have developed to the stage where wavefunctions of such quality can be readily obtained for a wide range of molecules, the situation is quite different for continuum molecular electronic states. The development of quantitative methods for obtaining the Hartree–Fock continuum orbitals associated with molecules has been slow. This has been primarily due to the difficulties associated with the non-central and non-local potentials of molecular ions. As we will see below, our approach for obtaining these electronic molecular continuum orbitals, an essential building block in our studies, is based on the use of Schwinger variational procedures to solve the collisional equations for the photoelectron. Such scattering solutions are needed in general to fully describe the photoionisation experiment including photoelectron angular distributions.

An outline of the paper is as follows. In the next section we discuss the Schwinger variational method which we use to obtain the electronic continuum orbitals needed in studies of molecular photoionisation. In Section 3 we present results of several applications of these methods to single-photon ionisation of molecules including $N_2$, CO, $CO_2$, $C_2N_2$ and $C_2H_2$. Some features of our theory of resonant multiphoton ionisation of molecules (Dixit and McKoy 1985) are outlined in Section 4. This is followed (Section 5) by a discussion of results of applications of this theory to resonant multiphoton ionisation processes in $H_2$.

## 2. Electronic Continuum Orbitals

Throughout these studies of molecular photoionisation the final ionised state wavefunction is generally obtained using the frozen-core Hartree–Fock (FCHF) approximation. In this approximation the final state is described by a single electronic configuration in which the ionic core orbitals are constrained to be identical to the Hartree–Fock orbitals of the neutral molecule and the photoelectron orbital satisfies the one-electron Schrödinger equation

$$\{-\tfrac{1}{2}\nabla^2 + V_{N-1}(r, R) - \tfrac{1}{2}k^2\}\phi_k(r, R) = 0, \tag{1}$$

where $\frac{1}{2}k^2$ is the photoelectron kinetic energy and $\phi_k$ satisfies the appropriate boundary conditions. The key step in the study of molecular photoionisation is the determination of these Hartree–Fock continuum functions, $\phi_k$.

To obtain the continuum orbital $\phi_k$ it is convenient to work with the integral form of (1), i.e.

$$\phi_k(r) = \phi_k^{\mathrm{C}} + G_{\mathrm{C}}^{(-)} V \phi_k, \tag{2}$$

where $\phi_k^{\mathrm{C}}$ is the Coulomb scattering wavefunction and $V$ is the molecular ion potential $V_{N-1}$ with the Coulomb potential removed,

$$V = V_{N-1} + r^{-1}; \tag{3}$$

$G_{\mathrm{C}}^{(-)}$ is the Coulomb Green function with incoming-wave boundary conditions, i.e.

$$(-\tfrac{1}{2}\nabla^2 - r^{-1} - \tfrac{1}{2}k^2) G_{\mathrm{C}}(r, r') = -\delta(r - r'). \tag{4}$$

To solve (2) we expand $\phi_k$ in a partial wave series in angles about $k$

$$\phi_k(r) = (2/\pi)^{\frac{1}{2}} \sum_{l=0}^{l_{\mathrm{p}}} \sum_{m=-l}^{l} \mathrm{i}^l \psi_{klm}(r)\, Y_{lm}^*(\hat{k}). \tag{5}$$

Substitution of (5) into (2) shows that each $\psi_{klm}$ satisfies its own Lippmann–Schwinger equation

$$\psi_{klm}(r) = S_{klm} + G_{\mathrm{C}}^{(-)} V \psi_{klm}, \tag{6}$$

where $S_{klm}$ is a partial wave Coulomb function. In (5) an infinite sum over $l$ has been truncated at $l = l_{\mathrm{p}}$. This partial wave expansion of the scattering solution must obviously be truncated at a value of $l_{\mathrm{p}}$ large enough to ensure convergence of the resulting cross sections. Typical values of $l_{\mathrm{p}}$ are about 8–10 (Lucchese *et al.* 1982, 1986).

We have developed an iterative procedure for solving (6) which is based on the Schwinger variational method. Details of this procedure have been discussed elsewhere (Lucchese *et al.* 1986) and here we only outline a few essential features of the procedure. We first solve (6) for $\psi_{klm}$ by assuming an approximate separable form for the scattering potential $V$

$$V(r, r') \approx V^{\mathrm{S}}(r, r') = \sum_{i,j} \langle r | V | \alpha_i \rangle (V^{-1})_{ij} \langle \alpha_j | V | r' \rangle, \tag{7}$$

where the matrix $(V^{-1})_{ij}$ is the inverse of the matrix with elements $V_{ij} = \langle \alpha_i | V | \alpha_j \rangle$ and $|\alpha_i\rangle$ is a member of a basis set. With this separable approximation to $V$, the solutions of (6) are

$$\psi_{klm}^{(0)}(r) = S_{klm}(r) + \sum_{i,j} \langle r | G_{\mathrm{C}}^{(-)} V | \alpha_i \rangle (D^{-1})_{ij} \langle \alpha_j | V | S_{klm} \rangle, \tag{8}$$

where the matrix $(D^{-1})_{ij}$ is the inverse of the matrix with elements

$$D_{ij} = \langle \alpha_i | V - V G_C^{(-)} V | \alpha_j \rangle. \tag{9}$$

This solution $\psi^{(0)}_{klm}$ can be shown to be equivalent to the use of the basis $|\alpha_i\rangle$, $i = 1, \ldots, N$ in the Schwinger variational principle for the $T$-matrix (see e.g. Miller 1969), i.e. we can write (8) as

$$\psi^{(0)}_{klm}(r) = S_{klm}(r) + G_C^{(-)} T^{(0)} | S_{klm} \rangle, \tag{10}$$

where $T^{(0)}$ is variationally stable. We note that in this equation $\psi^{(0)}_{klm}$ is now uncoupled, i.e. if we further expand $\psi^{(0)}_{klm}(r)$ as

$$\psi^{(0)}_{klm}(r) = \sum_{l'm'} g_{lm:\, l'm'}(k, r)\, Y_{l'm'}(\hat{r}), \tag{11}$$

substitute this expansion into (10), and then project with the spherical harmonics, the resulting equations for $g_{lm:\, l'm'}$ are uncoupled and can be readily solved by numerical quadrature. For linear molecules we have $m = m'$.

The functions $\alpha_i(r)$ used in (7) can be chosen to be entirely discrete basis functions such as cartesian gaussian (see e.g. Dunning and Hay 1977), spherical gaussian (Lucchese and McKoy 1982*a*), or Slater functions. These discrete basis functions have been used successfully in electronic structure calculations and are known to be effective in representing the multicentre nature of the scattering wavefunction and molecular potential in the near-molecular region. It is very important to note that with discrete basis functions only in (8) the approximate solutions $\psi^{(0)}_{klm}$ satisfy scattering boundary conditions associated with the $T$-matrix $T^{(0)}$. Of course, this is a consequence of working with the integral equation for the scattering wavefunction. With adequate basis sets the continuum solutions $\psi^{(0)}_{klm}$ already provide quantitatively reliable photoionisation cross sections which, moreover, can be shown to be variationally stable at the Hartree–Fock level (Lucchese and McKoy 1983). For some applications (Lucchese and McKoy 1983; Dixit *et al.* 1985), the converged solutions of (6) may be required. We recall that $\psi^{(0)}_{klm}$ is only a solution of (6) in which $V$ has been approximated by $V^S$. To obtain these solutions we have developed an iterative technique for solving (6) starting with the solutions $\psi^{(0)}_{klm}$. In this procedure (Lucchese *et al.* 1980, 1986) these approximate numerical continuum solutions are viewed as new basis functions. We then add these numerical basis functions to our original discrete basis set to form a new and larger basis. This new expanded basis is then used in (8) to obtain an improved approximation $\psi^{(1)}_{klm}$ to $\psi_{klm}$. By continuing this procedure iteratively we can obtain systematically more accurate solutions to (6). Conditions for assessing the convergence of this iterative Schwinger variational method have been discussed (Lucchese *et al.* 1986; Lucchese and McKoy 1982*a*). With good initial basis sets this iterative procedure can converge in one or two iterations.

All matrix elements and functions arising in our procedure are evaluated using single-centre expansions truncated at some suitable maximum value. The convergence of these cross sections with respect to the expansion parameters has been studied (Lucchese *et al.* 1986). The associated radial integrals are evaluated using a Simpson's rule quadrature (Lucchese *et al.* 1986).

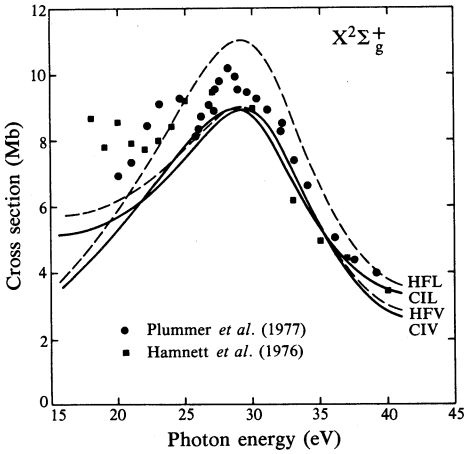


**Fig. 1.** Photoionisation cross section for production of the $X^2\Sigma_g^+$ state of $N_2^+$ with different initial state wavefunctions (1 Mb = $10^{-18}$ cm$^2$).

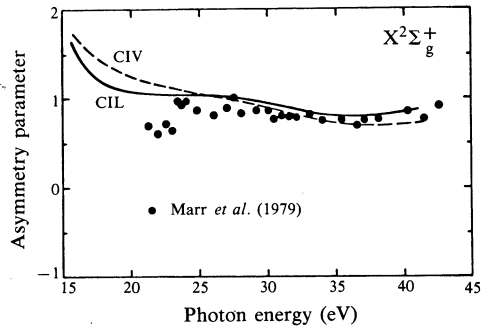


**Fig. 2.** Photoelectron asymmetry parameters for the $X^2\Sigma_g^+$ state of $N_2^+$ using a CI initial state wavefunction.

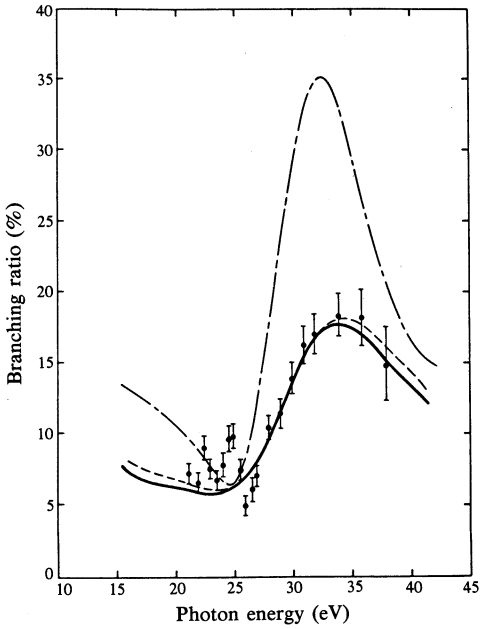


**Fig. 3.** Vibrational branching ratios for the $\nu' = 1$ to $\nu' = 0$ levels of the $X^2\Sigma_g^+(3\sigma_g^{-1})$ state of $N_2^+$:
—— FCHFL results;
– – – FCHFV results;
—·— multiple scattering results (Dehmer *et al.* 1979);
• experimental data (West *et al.* 1980).

## 3. Single-photon Studies

We will now discuss the results of applications of the above procedure to study the role of shape and autoionising resonances on the photoionisation cross sections in several molecules. Shape and autoionising resonances lead to many important and prominent features in molecular photoionisation spectra including non-Franck–Condon ionic vibrational-state distributions and a vibrational-state dependence in the photoelectron asymmetry parameters. Shape resonances are quasibound states formed by the trapping of the photoelectron by the centrifugal barrier of the molecular force field. The centrifugal barriers of molecular force fields can involve very high angular momentum character. Such resonances are essentially one-electron in nature with charge densities primarily localised in the molecular core region and hence these properties are to a great extent determined by the molecular core potential. These characteristics of shape resonances, along with the expected strong dependence of the wavefunction on energy and internuclear distance near the resonance, suggest that they should be studied using realistic molecular potentials and electronic continuum states. In our studies of these resonances we will use the Hartree–Fock electronic continuum states of the molecular ion to describe the photoelectron.

As a first example we discuss the well-known shape resonance feature which occurs in photoionisation out of the $3\sigma_g$ level of $N_2$ leading to the $X^2\Sigma_g^+$ state of $N_2^+$. This shape resonant behaviour occurs in the $3\sigma_g \rightarrow k\sigma_u$ channel and has been studied extensively by several methods (Davenport 1976; Rescigno *et al.* 1978; Lucchese *et al.* 1982). Our calculated cross sections (Lucchese *et al.* 1982) using both Hartree–Fock (HF) and configuration interaction (CI) initial state wavefunctions and the length (L) and velocity (V) forms of the oscillator strength are shown in Fig. 1. In all cases the final state wavefunction is obtained in the FCHF approximation. These results show that the calculated cross sections agree quite well with available experimental data (Hamnett *et al.* 1976; Plummer *et al.* 1977) and that inclusion of initial-state correlation effects reduces the difference between the length and velocity forms of the cross section. Differences between the length and velocity forms of these cross sections are known to provide a measure of the role of electron correlation in the photoionisation process. The differences between these calculated results and the measured cross sections around 23 eV are primarily due to autoionisation, the effects of which are not included in the FCHF model. In Fig. 2 we show our calculated photoelectron asymmetry parameters, which define the photoelectron angular distributions (McKoy *et al.* 1984) for the $X^2\Sigma_g^+$ state of $N_2^+$ along with the measured values (Marr *et al.* 1979). The agreement with the experimental data is good, except for energies below 23 eV where autoionisation is important.

Fig. 3 shows the calculated and experimental branching ratios for the $\nu' = 1$ to $\nu' = 0$ levels for photoionisation leading to the $X^2\Sigma_g^+(3\sigma_g^{-1})$ state of $N_2^+$ (Lucchese and McKoy 1981). In the Franck–Condon approximation this branching ratio should be independent of photon energy and should for this system have a Franck–Condon value, expressed as a percentage, of 7·86. The non-Franck–Condon behaviour of this branching ratio, first predicted by Dehmer *et al.* (1979), arises from the strong dependence of the photoelectron matrix element on internuclear distance in the resonance region. Our calculated branching ratios agree well with the experimental data of West *et al.* (1980) except for the autoionising structure around 23 eV. It is important to note that substantial non-Franck–Condon behaviour occurs in these

branching ratios at photon energies well above the resonance peak position of about 29 eV.

Fig. 4 shows the fixed-nuclei photoionisation cross sections for the $5\sigma$ level of CO obtained using a Hartree–Fock wavefunction for the initial state and the FCHF approximation for the final state (Lucchese and McKoy 1983). In analogy to $N_2$, these cross sections show shape resonant behaviour in the $k\sigma$ continuum. We note, however, that the resonant feature is considerably broader in CO than in $N_2$. In Fig. 4 we also show the calculated cross sections obtained using the Stieltjes moment theory method (STMT) (Padial *et al.* 1978) and the multiple scattering model (Davenport 1976) along with the experimental results of Hamnett *et al.* (1976) and Plummer *et al.* (1977). The STMT cross sections, which were also obtained in the FCHF approximation, seem to indicate that the feature at 24 eV in the experimental data is due to the $k\sigma$ shape resonance, whereas the present results suggest that it arises from autoionisation (Stephens *et al.* 1981).

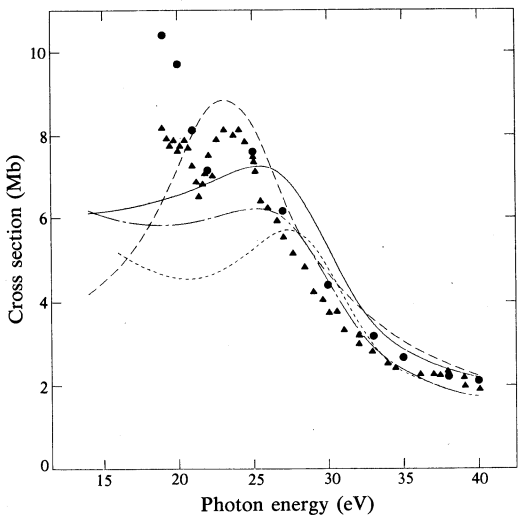


**Fig. 4.** Photoionisation cross sections for production of the $X^2\Sigma^+(5\sigma^{-1})$ state of $CO^+$:
—— FCHFL results;
—·— FCHFV results;
----- multiple scattering results (Davenport 1976);
– – – STMT results (Padial *et al.* 1978);
• Hamnett *et al.* (1976);
▲ Plummer *et al.* (1977).

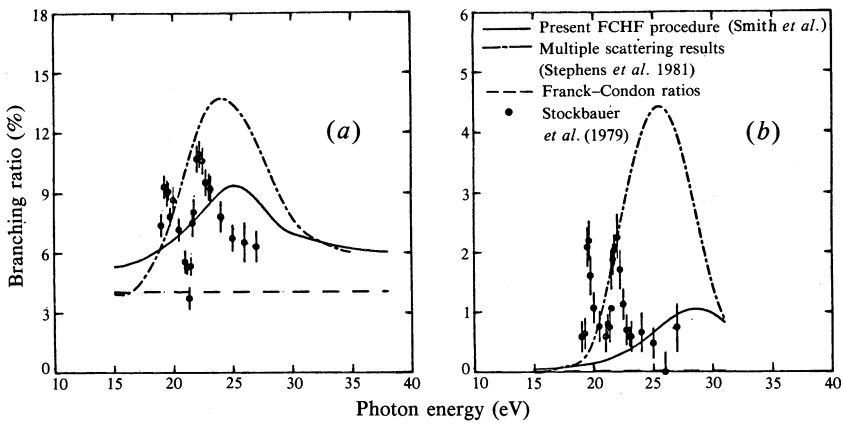


**Fig. 5.** Branching ratios for (*a*) the $v = 1$ to $v = 0$ and (*b*) the $v = 2$ to $v = 0$ vibrational levels in photoionisation of the $5\sigma$ level of CO.

Fig. 5 shows the $v = 1$ to $v = 0$, and $v = 2$ to $v = 0$ vibrational branching ratios for photoionisation out of the $5\sigma$ orbital of CO. From these results we see that, although the shape resonance does give rise to non-Franck–Condon vibrational branching ratios, the pronounced non-Franck–Condon behaviour seen experimentally is not due to the shape resonance. In fact, what we seem to have in this energy region is structure in the vibrational branching ratios arising from both an autoionising and a shape resonance. Measurements of these branching ratios, particularly those for the $v = 2$ to $v = 0$ levels, at higher photon energies would clearly be helpful.

A shape resonance in the $k\sigma_u$ continuum also plays an important role in the photoionisation of $CO_2$. This resonant feature appears prominently in photoionisation out of the $1\pi_g$, $4\sigma_g$ and $1\sigma_g$ orbitals. Fig. 6 shows the fixed-nuclei and vibrationally averaged cross sections obtained by the present procedure (Lucchese and McKoy 1982*a*) and by the continuum multiple scattering model, CMSM (Swanson *et al.* 1980) along with the fixed-nuclei results of the STMT method (Padial *et al.* 1981) for photoionisation of the $4\sigma_g$ orbital of $CO_2$. The vibrational averaging of these cross sections is carried out over the symmetric stretching mode only. There are very clear differences between the cross sections given by the various methods. The CMSM leads to a very narrow resonance with a peak value which is dramatically reduced by vibrational averaging. On the other hand, the effect of vibrational averaging on the FCHF cross sections is much less. This resonant feature is, furthermore, essentially not evident in the STMT results which are in better apparent agreement with the experimental data (Brion and Tan 1978; see also Roy *et al.* 1984). It is important to realise that the present cross sections and those of the STMT calculations should be equivalent since both results are obtained within the FCHF approximation (Lucchese and McKoy 1982*b*). Possible reasons why the moment theory procedure does not show the resonance feature have been discussed elsewhere (Lucchese and McKoy 1982*b*). This resonant behaviour is, however, quite pronounced in the photoelectron asymmetry parameters which are shown in Fig. 7 (Katsumata *et al.* 1979; Carlson *et al.* 1981). These results show that several important features of these $4\sigma_g$ cross sections are not yet understood.

To examine the role of shape resonances in a larger polyatomic system we now look at the photoionisation of the $5\sigma_g$ orbital of $C_2N_2$ (Lynch *et al.* 1986). The possibility of shape resonant trapping in this molecule can be quite interesting due to the C≡N groups and the C–C bond. Some line source studies (Kreile *et al.* 1983) and synchrotron radiation measurements (Holland *et al.* 1983) of these cross sections below a photon energy of 24 eV have been reported. The CMSM has also been used to study both the photoionisation cross sections and photoelectron asymmetry parameters (Kreile *et al.* 1983). In Fig. 8 we show our calculated cross sections for photoionisation of the $5\sigma_g$ level leading to the $\tilde{A}^2\Sigma_g^+$ state of $C_2N_2^+$ along with the individual contributions from the $\sigma_u$ and $\pi_u$ continua. These cross sections along with their eigenphase sums, which are not shown here, show that there is a low and higher energy shape resonance in the $\sigma_u$ continuum and an additional shape resonance in the $\pi_u$ channel. The low energy $\sigma_u$ resonance is well-known to be the C–C analogue of the $\sigma_u$ ($l = 3$) shape resonance in $N_2(3\sigma_g^{-1})$ (Holland *et al.* 1983). The higher energy $\sigma_u$ resonance shows substantial mixing among the $l = 3, 5, 7$ partial waves, suggesting that the photoelectron wavefunction has significant amplitude in the region of the C≡N subgroups. This shape resonance is just the $\sigma_u$ combination of shape resonances localised on the CN groups (Holland *et al.* 1983). Finally, to

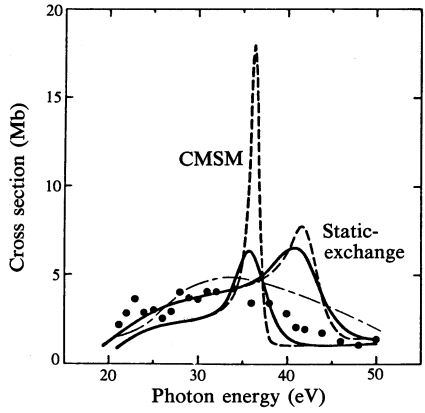


**Fig. 6.** Photoionisation cross sections leading to the $C^2\Sigma_g^+(4\sigma_g^{-1})$ state of $CO_2^+$:
- - - - fixed-nuclei cross sections, obtained by the present FCHF procedure and the CMSM (Swanson *et al.* 1980);
——— cross sections averaged over the symmetric stretching mode, obtained by the present FCHF procedure and the CMSM (Swanson *et al.* 1980);
—·—·— STMT fixed nuclei results (Padial *et al.* 1981);
• experimental data (Brion and Tan 1978).

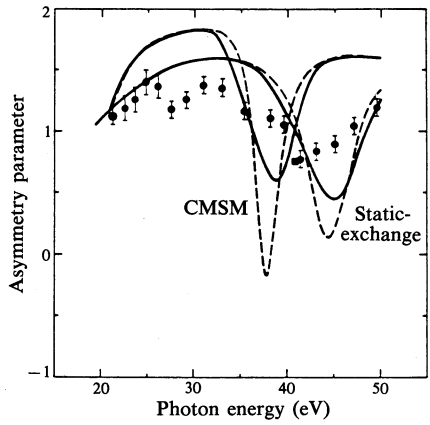


**Fig. 7.** Photoelectron asymmetry parameters for photoionisation of the $4\sigma_g$ orbital of $CO_2$:
- - - fixed-nuclei results;
——— averaged over the symmetric stretching mode;
• experimental data (Carlson *et al.* 1981);
▪ experimental data (Katsumata *et al.* 1979).

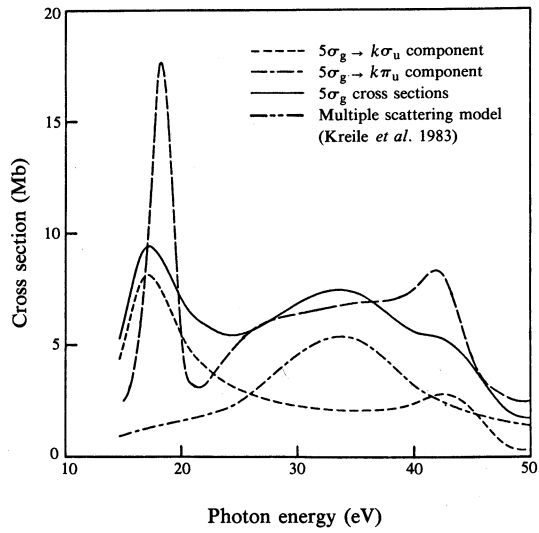


**Fig. 8.** Photoionisation cross sections for the $5\sigma_g$ orbital leading to the $\tilde{A}^2\Sigma_g^+$ state of $C_2N_2^+$.

our knowledge, the occurrence of a shape resonance in the $5\sigma_g \rightarrow k\pi_u$ channel is unusual and has not been seen in studies of other linear molecules.

To date most studies of molecular photoionisation have been carried out in the FCHF approximation. In this approximation the ionic core orbitals are constrained to be identical to those of the neutral molecule and the photoelectron orbital is determined in the field of this unrelaxed core. This sudden approximation completely neglects any restructuring of the molecular core upon ionisation and should be more appropriate for photoionisation of valence levels than of the deeper or K-shell levels. The presence of a shape resonance in the cross sections can make this approximation even poorer than expected.

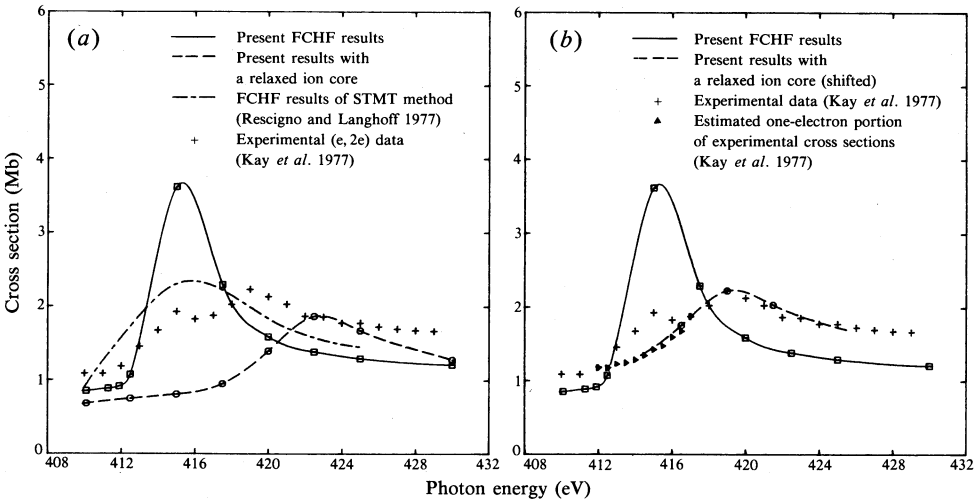


**Fig. 9.** The K-shell photoionisation cross sections for $N_2$. In (*b*) the present results with a relaxed ion core have been shifted so that the peak position coincides with that of the experimental cross section.

As our next example, we look at the important role of core relaxation on the shape-resonant K-shell photoionisation cross sections in $N_2$. In Fig. 9*a* we show our calculated frozen-core cross sections for K-shell photoionisation for $N_2$ (Lynch and McKoy 1984) along with the results obtained previously using the STMT method (Rescigno and Langhoff 1977) and the experimental data (Kay *et al.* 1977). These cross sections include contributions from the nearly degenerate $1\sigma_g$ and $1\sigma_u$ levels. The present frozen-core results differ significantly from the experimental data. The $\sigma_u$ resonance feature is quite strongly peaked and concentrates much of the cross section too close to threshold. On the other hand, the frozen-core cross sections of the STMT method show a much broader resonance feature and are apparently in better agreement with the measured cross sections. As discussed elsewhere (Lynch and McKoy 1984), a probable explanation for the difference between our results and those of the STMT method is that the pseudo-spectrum used in these STMT studies did not have a sufficiently dense distribution of poles in the resonance region. This can lead to a broadening of the resonance structure. Fig. 9*a* also shows the K-shell cross sections obtained using a relaxed HF ionic core and the corresponding

continuum orbitals. Although the assumption that the photoelectron moves in the field of such a completely relaxed ion is not rigorous, applications to atomic inner-shell photoionisation have shown that it is a very reasonable model. These results show that core relaxation has decreased the cross section near threshold dramatically, broadened the resonance, and shifted it to higher energy. The resonance position is now at too high an energy suggesting that the model of a completely relaxed ionic core has led to excessive screening of the hole. However, the general shape of the relaxed-core cross sections is quite similar to that of the experimental data and to illustrate this, Fig. 9*b* shows these cross sections for a limited range of photon energy shifted so that their peak position coincides with that of the measured cross sections.

In addition to shape resonances, autoionising resonances play an important role in molecular photoionisation spectra. As an example we will look at the pronounced

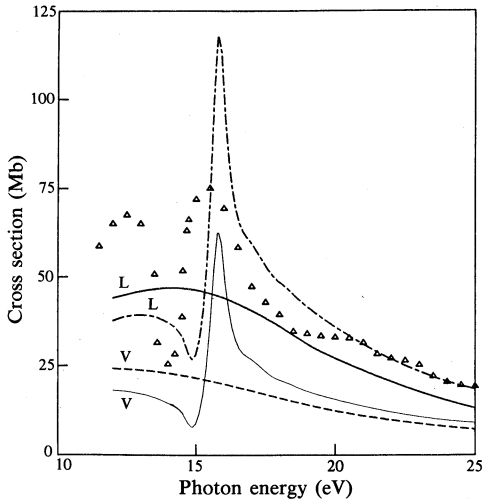


**Fig. 10.** Photoionisation cross sections for the $X^2\Pi_u(1\pi_u^{-1})$ state of $C_2H_2^+$:
——, - - - - results without autoionisation for the L and V forms;
– – –, —— results including the $2\sigma_u 1\pi_g$ autoionising resonance for L and V forms;
△ experimental data from Langhoff *et al.* (1981) normalised to the calculated cross sections (L) including autoionisation at 24 eV.

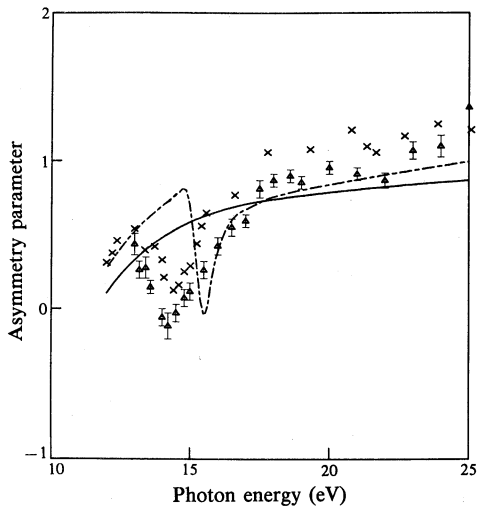


**Fig. 11.** Photoelectron asymmetry parameters for the $X^2\Pi_u$ state of $C_2H_2^+$, showing
—— present results without autoionisation (L form);
– – – present results including autoionisation (L form);
△ data from Parr *et al.* (1982);
× data from Keller *et al.* (1982).

double-bump structure seen around 14 eV in photoionisation of the $1\pi_u$ orbital of $C_2H_2$. In spite of several recent theoretical (Kreile *et al.* 1981; Machado *et al.* 1982; Levine and Soven 1983; Lynch *et al.* 1984) and experimental (Kreile *et al.* 1981; Unwin *et al.* 1981; Parr *et al.* 1982; Keller *et al.* 1982) studies, we do not as yet have a definitive quantitative understanding of the underlying resonance structure in this region, for example, to what extent the structure is due to shape or autoionising resonances or to some combination of such resonances. Of these studies, those of Levine and Soven (1983) are the most relevant to the results we now discuss. Using a time-dependent local-density approximation, they have identified the structure in the 12–17 eV region as arising from an autoionising $2\sigma_u \rightarrow 1\pi_g$ resonance and a redistribution of oscillator strength from a discrete $1\pi_u \rightarrow 1\pi_g$ transition to the continuum. Figs 10 and 11 show the results of our present studies of this feature in the photoionisation spectrum of acetylene. In these studies we used the CI formalism of Fano (1961) to couple the discrete $2\sigma_u\, 1\pi_g(^1\Pi_u)$ state to the background continuum for photoionisation of the $1\pi_u$ orbital. We used the improved virtual orbital (IVO) model (Goddard and Hunt 1974) to obtain the resonance $1\pi_g$ orbital and Hartree–Fock orbitals for the background continuum. We note that this resonance state couples only to the $1\pi_u\, k\sigma_g$ and $1\pi_u\, k\delta_g(^1\Pi_u)$ continuum and not to the $1\pi_u\, k\pi_g(^1\Sigma_u)$. Furthermore, we did not include correlation effects in the background $^1\Sigma_u^+$ continuum. These $1\pi_u \rightarrow k\pi_g(^1\Sigma_u^+)$ cross sections will be strongly influenced by electron correlation which, in turn, will lead to a redistribution of oscillator strength in this region. The measured cross sections are not absolute and are normalised to our results at 24 eV. The resonant feature in these fixed-nuclei studies is narrower with a much larger peak value than seen experimentally. Inclusion of electron correlation in the resonant wavefunction, e.g. the $2\sigma_g\, 2\sigma_u^2\, 1\pi_g^2\, 3\sigma_g^2\, 1\pi_u^3$ configuration, should reduce the cross section in the resonance region. Vibrational averaging of these cross sections associated with a valence-like autoionising state will also broaden the feature. Details of these calculations will be discussed elsewhere (Lynch *et al.* 1986). It is worth noting, however, that our results imply that this feature arises from an autoionising resonance imposed on a shape resonance in the $k\pi_g$ continuum. This view differs from that of Levine and Soven (1983) where, in the absence of correlation, the $1\pi_u \rightarrow k\pi_g$ cross sections are small. Correlation will certainly reduce the oscillator strength assumed here for the $2\sigma_u \rightarrow 1\pi_g$ excitation and redistribute the $1\pi_u \rightarrow k\pi_g$ oscillator strength distribution to lower energy and into the discrete spectrum. Measurements of the absolute cross sections in this spectral region would be very helpful in sorting out the detailed dynamics of this feature. Finally, to our knowledge, these results are the first non-empirical studies of an autoionising resonance in a polyatomic molecule.

Angle-resolved photoelectron spectroscopy (ARPES) has evolved into a powerful probe of adsorbate–substrate systems (see e.g. Plummer and Gustafsson 1977). This technique provides information concerning both site geometry and bonding character. For example, ARPES can help determine adsorbate alignment and orbital symmetries associated with photoelectron spectra. The prototype adsorbate–substrate system for ARPES studies has been CO on Ni. Very early studies of ARPES in this system assumed that the only role of the surface was to orient the molecule and hence an oriented CO molecule was taken as a model for adsorbed CO (Davenport 1976). For orbitals not directly involved in bonding to the surface, e.g., $4\sigma$ and $1\pi$, this is a good approximation and gives qualitative agreement with experimental data.

However, oriented CO is a poor model for the $5\sigma$ orbital which is directly involved in bonding to the metal surface. For such orbitals, and quite generally, studies have shown that local cluster models, e.g. NiCO, $NiN_2$ and NiCO, can be good models of chemisorption to metals (see e.g. Kao and Messmer 1985). Studies of photoelectron angular distributions from such oriented cluster models can be expected to be more realistic models of photoemission from adsorbates and to reflect some of the effects of adsorbate–substrate bonding.

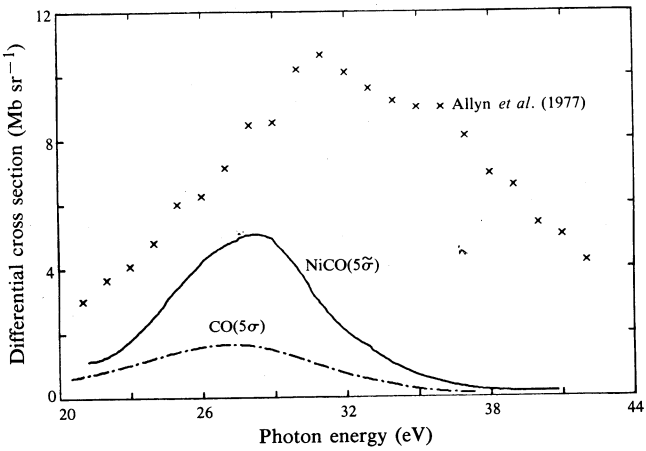


**Fig. 12.** Photon energy dependence of the photoemission cross section for $(\theta_p, \phi_p) = (45°, 0°)$ and $(\theta_k, \phi_k) = (0°, 0°)$. The experimental data of Allyn *et al.* (1977) are normalised as discussed below.

As a first step in this direction, we have studied the photoelectron angular distributions from the oriented molecular fragment NiCO and details of these studies will be given elsewhere (Dubs *et al.* 1986). However, we note here that we used a Hartree–Fock wavefunction for the initial state of NiCO assuming a $d^{10}$ configuration for Ni and FCHF continuum orbitals in the final state. In Fig. 12 we show results of the $5\sigma$ orbital of oriented CO and of the $5\sigma$-like ($5\tilde{\sigma}$) level of oriented NiCO along with the experimental data of Allyn *et al.* (1977). In this experiment polarised light was used $[(\theta_p, \phi_p) = (45°, 0°)]$ and photoelectrons were collected normal to the surface $[(\theta_k, \phi_k) = (0°, 0°)]$. Although the data include flux from both the $5\tilde{\sigma}$ and $1\tilde{\pi}$ levels, the contribution from the $1\tilde{\pi}$ orbital is expected to be negligible for collection along the molecular axis. Furthermore, the experimental data have been normalised in magnitude by setting the peak value of the measured $4\tilde{\sigma}$ cross section (Allyn *et al.* 1977) equal to our calculated values for the NiCO $4\tilde{\sigma}$ orbital. The calculated CO $5\sigma$ cross sections are also shifted down by 0·5 eV so as to compare the $5\sigma$(CO) and $5\tilde{\sigma}$(NiCO) cross sections at the same photoelectron kinetic energy. The magnitude of the NiCO cross section is in somewhat better agreement with the experimental data for CO on Ni. This difference in cross section reflects the bonding of the $5\sigma$ orbital of CO to Ni. The experimental peak is considerably broader than that of NiCO($5\tilde{\sigma}$) and is also shifted to higher energy. Additional results of these studies of photoemission of oriented NiCO will be published elsewhere (Dubs *et al.* 1986).

## 4. Multiphoton Studies

As discussed earlier, resonant enhanced multiphoton ionisation (REMPI) of molecules, coupled with kinetic energy analyses of the photoelectrons, is emerging as a powerful probe of neutral intermediate states (Pratt *et al.* 1983) and of the photoionisation dynamics of excited states (Pratt *et al.* 1984*b*). In recent years there has been an upsurge of experimental activity in REMPI studies of diatomic and small polyatomic molecules (Kimura 1985) which have demonstrated important dynamical features such as Rydberg-valence mixing, striking non-Franck–Condon behaviour, and state-selective production of ions.

In spite of the increasing availability of such data, there has been little quantitative theoretical work on the understanding of the dynamical features observed in these experiments (Kimura 1985). The theoretical analyses of REMPI of these systems is non-trivial with complexities arising from the multiphoton nature of the process and from the molecular aspects themselves. In addition to the need for a theoretical framework for carrying out quantitative studies of REMPI processes, such studies require reliable molecular photoelectron continuum orbitals over a limited energy range and for several internuclear distances.

Recently we have developed a theory for the analysis of REMPI processes in molecules (Dixit and McKoy 1985). Our approach consists of viewing the $(n+m)$-photon ionisation process from an isotropic initial state as $m$-photon ionisation out of an oriented, excited state. The orientation in this resonant state, which is reached by $n$-photon excitation from the initial state, is non-isotropic and is characteristic of the absorption process. The ionisation simply probes this anisotropic population. Our approach to the study of REMPI in molecules thus consists of determining the anisotropy created in the resonant state and then coupling this anisotropic population to ionisation out of it. The photoelectron orbitals of this final state are taken to be FCHF continuum orbitals. In applications, these continuum orbitals are obtained using the procedure outlined in Section 2.

As one of the first applications of this approach, we have analysed the vibrational branching ratios resulting from a $(3+1)$-resonant multiphoton ionisation of $H_2$ via the $C^1\Pi_u$ state (Dixit *et al.* 1984). The motivation for choosing this particular scheme of ionisation was the experiment of Pratt *et al.* (1984*b*) who analysed the photoelectron energy spectrum resulting from a three-photon resonant four-photon ionisation of $H_2$ via this state. The $v' = 0$–4 levels of the $C^1\Pi_u$ state are perturbed by various levels of the $B^1\Sigma_u^+$ state. However, the $C^1\Pi_u^-$ levels are unaffected by this perturbation. Since the Q branch accesses the $\Pi_u^-$ components, Pratt *et al.* (1984*b*) avoided the effects of these perturbations by tuning the laser frequency in resonance with the Q(1) line. This illustrates the tremendous selectivity achievable in resonant multiphoton ionisation. The actual process studied was

$$H_2(X^1\Sigma_g^+, v'', J_0=1) \xrightarrow{3h\nu} H_2^*(C^1\Pi_u, v', J_i=1) \xrightarrow{h\nu} H^+(X^2\Sigma_g^+, v^+)+e^- . \qquad (12)$$

Fig. 13 shows the measured vibrational branching ratios for ionisation out of the $v' = 0$–4 levels of the $C^1\Pi_u$ state into vibrational levels $v^+$ of the ion. These branching ratios deviate significantly from the appropriate Franck–Condon factors. Possible causes for these deviations include the energy and internuclear dependence of the electronic transition moment, autoionisation, and perturbations with overlapping

transitions. Of these possibilities, accidental resonances and perturbations are known not to be important in this system (Pratt *et al.* 1984*b*).

In our studies we quantitatively assessed the role of the energy and internuclear dependence of the electronic transition moment on these vibrational ratios. Fig. 13 shows these branching ratios calculated at three different levels of approximation (Dixit *et al.* 1984): (i) the Franck–Condon approximation, i.e. no energy or internuclear dependence in the photoelectron matrix element; (ii) the non-Franck–Condon approximation, i.e. internuclear but no energy dependence in the photoelectron matrix element; (iii) full internuclear and energy dependences in the matrix element.

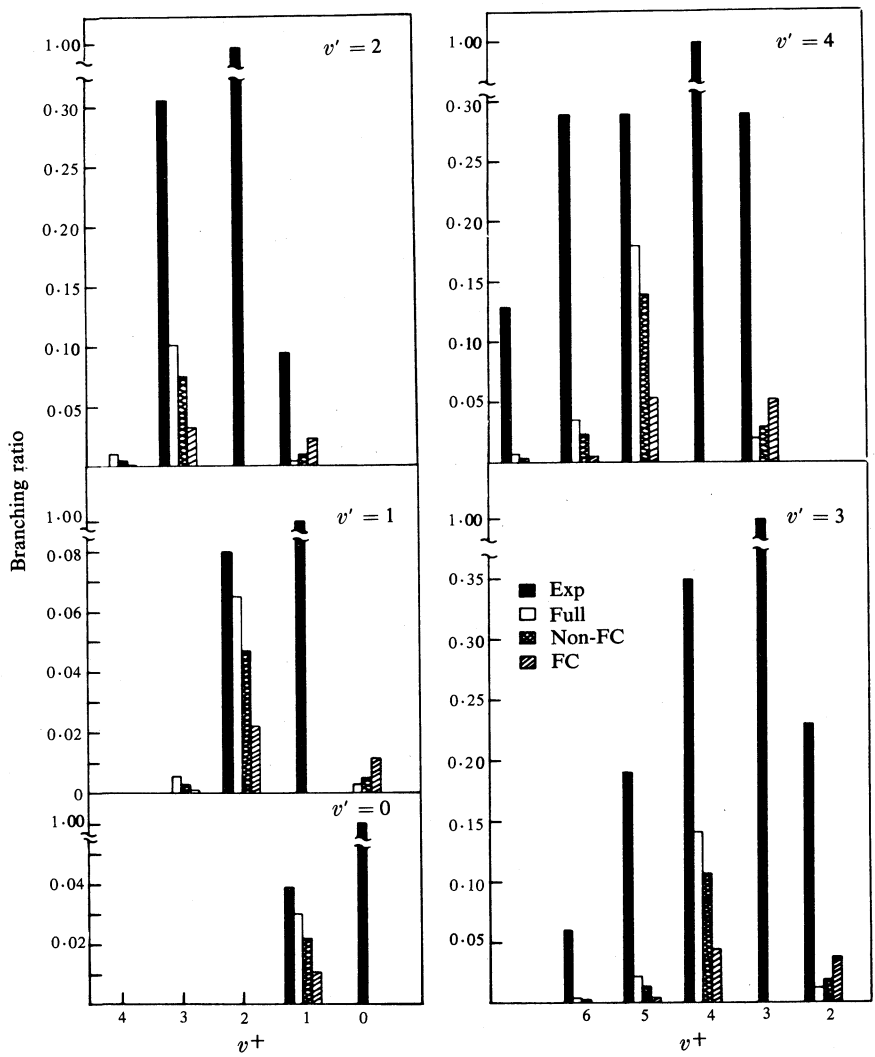


**Fig. 13.** Vibrational branching ratios in (3+1) REMPI of $H_2$ via the $C^1\Pi_u$ state; $v'$ denotes the vibrational state of the $C^1\Pi_u$ state and $v^+$ that of the $X^2\Sigma_g^+$ state of $H_2^+$. The results are normalised so that the $v' = v^+$ peak in all three approximations and in the experiment is of unit height (note the break in the graph for the $v' = v^+$ peak).

The results in Fig. 13 show that the energy and internuclear dependence of the electronic transition moment are important elements in this non-Franck–Condon behaviour. For the $v' = 0$ and 1 excitations, agreement between theory and experiment seems quite good. For the $v' = 2$–4 excitations, the experimental branching ratios for $v^+ \neq v'$ are much larger than the theoretical predictions. In particular, for $v' = 4$, the $v^+ = 3, 5, 6$ experimental peaks are all of about equal height, while theory predicts the heights of the $v^+ = 3$ and 6 peaks to be less than that of the $v^+ = 5$ peak by a factor of 0·11 and 0·2 respectively. A similar discrepancy exists in the $v' = 3$ and 2 excitation data as well. Further studies of these branching ratios are needed to understand their underlying dynamical origin.

## Acknowledgments

The material presented here was based upon research supported by the Chemical Physics Program of the Division of Chemistry of the National Science Foundation. One of us (R.L.D.) acknowledges support from a National Science Foundation Predoctoral Research Fellowship.

## References

Allyn, C. J., Gustafsson, T. L., and Plummer, E. W. (1977). *Chem. Phys. Lett.* **47**, 127.
Anderson, S. L., Kubiak, G. D., and Zare, R. N. (1984). *Chem. Phys. Lett.* **105**, 22.
Bjerre, N., Kachru, R., and Helm, H. (1985). *Phys. Rev.* A **31**, 1206.
Brion, C. E., and Tan, K. H. (1978). *Chem. Phys.* **34**, 141.
Burns, A. R. (1985). *Phys. Rev. Lett.* **55**, 525.
Carlson, T. A., Krause, M. O., Grimm, F. A., Allen, J. D., Jr, Mehaffy, D., Keller, P. R., and Taylor, J. W. (1981). *Phys. Rev.* A **23**, 3316.
Davenport, J. W. (1976). *Phys. Rev. Lett.* **36**, 945.
Dehmer, J. L., Dill, D., and Parr, A. C. (1984). *In* 'Photophysics and Photochemistry in the Vacuum Ultraviolet' (Eds S. McGlynn *et al.*), pp. 341–408 (Reidel: Dordrecht).
Dehmer, J. L., Dill, D., and Wallace, S. (1979). *Phys. Rev. Lett.* **43**, 1005.
Dixit, S. N., Lynch, D. L., and McKoy, V. (1984). *Phys. Rev.* A **30**, 3332.
Dixit, S. N., Lynch, D. L., McKoy, V., and Huo, W. M. (1985). *Phys. Rev.* A **32**, 1267.
Dixit, S. N., and McKoy, V. (1985). *J. Chem. Phys.* **82**, 3546.
Dubs, R. L., Smith, M. E., and McKoy, V. (1986). Studies of angle-resolved photoelectron spectra (ARPES) from oriented NiCO—a model for adsorbed CO. *Phys. Rev.* B (submitted for publication).
Dunning, T. H., Jr, and Hay, P. J. (1977). *In* 'Methods of Electronic Structure Theory' (Ed. H. F. Schaeffer III), pp. 1–27 (Plenum: New York).
Fano, U. (1961). *Phys. Rev.* **124**, 1866.
Goddard, III, W. A., and Hunt, W. J. (1974). *Chem. Phys. Lett.* **24**, 464.
Hamnett, A., Stoll, W., and Brion, C. E. (1976). *J. Electron Spectrosc. Relat. Phenom.* **8**, 367.
Holland, D. M. P., Parr, A. C., Ederer, D. L., West, J. B., and Dehmer, J. L. (1983). *Int. J. Mass. Spectrom. Ion Phys.* **52**, 195.
Kao, C. M., and Messmer, R. P. (1985). *Phys. Rev.* B **31**, 4835.
Katsumata, S., Achiba, Y., and Kimura, K. (1979). *J. Electron Spectrosc. Relat. Phenom.* **17**, 229.
Kay, R. B., van der Leeuw, Ph. E., and van der Wiel, M. J. (1977). *J. Phys.* B **10**, 2513.
Keller, P. R., Mahaffy, D., Taylor, J. W., Grimm, F. A., and Carlson, T. A. (1982). *J. Electron Spectrosc.* **27**, 223.
Kimura, K. (1985). *Adv. Chem. Phys.* **60**, 161.
Kreile, J., Schweig, A., and Thiel, W. (1981). *Chem. Phys. Lett.* **79**, 547.
Kreile, J., Schweig, A., and Thiel, W. (1983). *Chem. Phys. Lett.* **100**, 351.
Langhoff, P. W., McKoy, B. V., Unwin, R., and Bradshaw, A. (1981). *Chem. Phys. Lett.* **83**, 270.
Levine, Z. H., and Soven, P. (1983). *Phys. Rev. Lett.* **50**, 2074.
Lucchese, R. R., and McKoy, V. (1981). *J. Phys.* B **14**, L629.

Lucchese, R. R., and McKoy, V. (1982*a*). *Phys. Rev.* A **26**, 1406.
Lucchese, R. R., and McKoy, V. (1982*b*). *Phys. Rev.* A **26**, 1992.
Lucchese, R. R., and McKoy, V. (1983). *Phys. Rev.* A **28**, 1382.
Lucchese, R. R., Raseev, G., and McKoy, V. (1982). *Phys. Rev.* A **25**, 2572.
Lucchese, R. R., Takatsuka, K., and McKoy, V. (1986). *Phys. Rep.* **131**, 147.
Lucchese, R. R., Watson, D. K., and McKoy, V. (1980). *Phys. Rev.* A **22**, 421.
Lynch, D. L., Dixit, S. N., and McKoy, V. (1986). *J. Chem. Phys.* **84**, 5504.
Lynch, D. L., Lee, M.-T., Lucchese, R. R., and McKoy, V. (1984). *J. Chem. Phys.* **80**, 1907.
Lynch, D. L., and McKoy, V. (1984). *Phys. Rev.* A **30**, 1561.
Lynch, D. L., McKoy, V., and Huo, W. M. (1986). Studies of autoionisation in the spectra of $C_2H_2$. *J. Chem. Phys.* (to be published).
McKoy, V., Carlson, T. A., and Lucchese, R. R. (1984). *J. Phys. Chem.* **88**, 3188.
Machado, L. E., Leal, E. P., Csanak, G., McKoy, B. V., and Langhoff, P. W. (1982). *J. Electron Spectrosc.* **25**, 1.
Marinero, E., Rettner, C. T., and Zare, R. N. (1982). *Phys. Rev. Lett.* **48**, 1323.
Marr, G. V., Morton, J. M., Holmes, R. M., and McCoy, D. G. (1979). *J. Phys.* B **12**, 43.
Miller, W. H. (1969). *J. Chem. Phys.* **50**, 407.
Padial, N., Csanak, G., McKoy, B. V., and Langhoff, P. W. (1978). *J. Chem. Phys.* **69**, 2992.
Padial, N., Csanak, G., McKoy, B. V., and Langhoff, P. W. (1981). *Phys. Rev.* A **23**, 218.
Parr, A. C., Ederer, D. L., West, J. B., Holland, D. M. P., and Dehmer, J. L. (1982). *J. Chem. Phys.* **76**, 4349.
Plummer, E. W., and Gustafsson, T. (1977). *Science* **198**, 165.
Plummer, E. W., Gustafsson, T., Gudat, W., and Eastman, D. E. (1977). *Phys. Rev.* A **15**, 2339.
Pratt, S. T., Dehmer, P. M., and Dehmer, J. L. (1983). *J. Chem. Phys.* **78**, 4315.
Pratt, S. T., Dehmer, P. M., and Dehmer, J. L. (1984*a*). *Chem. Phys. Lett.* **105**, 28.
Pratt, S. T., Dehmer, P. M., and Dehmer, J. L. (1984*b*). *J. Chem. Phys.* **80**, 1706.
Rescigno, T. N., Bender, C. F., McKoy, B. V., and Langhoff, P. W. (1978). *J. Chem. Phys.* **68**, 970.
Rescigno, T. N., and Langhoff, P. W. (1977). *Chem. Phys. Lett.* **51**, 65.
Roy, P. J., Nenner, I., Adam, M. Y., Delwiche, J., Hubin-Franskin, M. J., Lablanquie, P., and Roy, D. (1984). *Chem. Phys. Lett.* **109**, 607.
Smith, M. E., Lynch, D. L., and McKoy, V. (1986). Resonance effects in the $5\sigma$ photoionisation of CO. *J. Chem. Phys.* (submitted for publication).
Stephens, J. A., Dill, D., and Dehmer, J. L. (1981). *J. Phys.* B **14**, 3911.
Stockbauer, R., Cole, B. E., Ederer, D. L., West, J. B., Parr, A. C., and Dehmer, J. L. (1979). *Phys. Rev. Lett.* **43**, 757.
Swanson, R., Dill, D., and Dehmer, J. (1980). *J. Phys.* B **13**, L231.
Unwin, R., Khan, I., Richardson, N. V., Bradshaw, A. M., Cederbaum, L., and Domcke, W. (1981). *Chem. Phys. Lett.* **77**, 242.
West, J. B., Parr, A. C., Cole, B. E., Ederer, D. L., Stockbauer, R., and Dehmer, J. L. (1980). *J. Phys.* B **13**, L105.
White, M. G., Seaver, M., Chupka, W. A., and Colson, S. D. (1982). *Phys. Rev. Lett.* **49**, 28.
Winick, H., and Doniach, S. (1980). 'Synchrotron Radiation Research' (Plenum: New York).
Zewail, A. H. (1983). *Faraday Discuss. Chem. Soc.* **75**, 315.

Manuscript received 10 April, accepted 11 July 1986